Self-Powered Piezoionic Strain Sensor toward the Monitoring of Human Activities

*Yang Liu, Ying Hu, Jingjing Zhao, Guan Wu, Xiaoming Tao, and Wei Chen**

Y. Liu, Dr. Y. Hu, J. Zhao, G. Wu, Prof. W. Chen

i-Lab, Suzhou Institute of Nano-tech and Nano-bionics

Chinese Academy of Sciences

Suzhou 215123 , P. R. China

E-mail: wchen2006@sinano.ac.cn

Prof. X. Tao

Nanotechnology Center

Institute of Textiles and Clothing

The Hong Kong Polytechnic University

Hong Kong SAR

Abstract

Wearable sensors for the detection of human activities including subtle physiological signals and large-scale body motion as well as distinguishing the motion direction are highly desirable, but still a challenge. A flexible wearable piezoionic strain sensor based on the ionic polymer membrane sandwiched between two conductive electrodes is developed. This ionic polymer sensor can generate electrical signal output (≈mV) with rapid response (≈50 ms) under the applied bending deformation due to the internal mobile ion redistribution. Compared with the currently studied resistive and capacitive sensors, this sensor can generate sensing signals without the requirement of additional power supply, and is able to distinguish the direction of the bending strain by observing the direction of generated electrical signals. For the sensor with metallic electrode, an output voltage of 1.3 mV is generated under a bending-induced strain of 1.8%, and this voltage can be largely increased when replacing the metallic electrodes by graphene composites. After simple encapsulation of the piezoionic sensor, a wearable sensor is

constructed and succeeded in monitoring the diverse human activities ranging from complex large scale multidimensional motions to subtle signals, including wrist bending with different directions, sitting posture sensing, pulse wave, and finger touch.

1. Introduction

Wearable strain sensors, which could capture and distinguish diverse human activities, are fascinating for their excellent features and have great potential applications related to the motion capture, health care, military, and friendly human- machine interaction system.[1–7] They can be integrated into cloth or directly attached on the human skin for the real-time monitoring of the human joint motions or physiological signals such as heartbeat and pulse wave. Therefore, there is an increasing demand for the development of the portable, wearable strain sensors.

Conventional studied wearable strain sensors are mainly resistive and capacitive types. They usually work by detecting the resistance as well as capacitance change of the materials in response to the external strain. Various resistive and capacitive sensors with novel materials and structures have been greatly developed, showing high sensitivity, good stability, and outstanding wearable performance toward human motion detection.[8–15] However, it is a little difficult to distinguish the upward-bending and the downward-bending for the typical resistive or capacitive sensor structure without asymmetrical design.[14,15] In other words, the direction of the bending-induced strain cannot be easily identified when the amplitude of the strain are the same, which is not beneficial for the detection of complexly multidimensional motions. The requirement of additional power supply for the operation of the sensors also affects the simplicity and integration of the sensor devices system. Moreover, achieving monitoring of both the large scale body motions and subtle physiological signals still remains challenge for the currently wearable sensor. Therefore, it is highly desirable to develop new type of wearable sensors to fulfill these urgent requirements.

Piezoionic effect materials refer to a class of ionic polymer composites which can generate electrical output in response to mechanical deformation with the mechanism of the ions redistribution.[16] In these materials, the inside mobile ions are moved in response to the external deformation, which is possibly due to the ion concentration gradients caused Donnan potential in the conductive polymer[17–20] or the imposed differential stress within the thickness of the membrane in the ionic polymer metal composites (IPMCs).[21–23] Compared with the widely studied piezoelectric and tribo-electric materials which can also convert mechanical energy into electrical power, the key difference lies in that the piezoionic effect is based on the mobile charged ions, unlike the dielectric charges in piezoelectric effect or contact electrification induced charges in triboelectric effect.[24–28] As one of the typical piezoionic materials, ionic polymer metal composite has extensively been studied during the last several years due to the excellent properties and potential applications in the areas of sensors and actuators.[23,29–36] It consists of a thin ionic polymer membrane with the noble metal electrodes coated on its two sides. The polymer membrane contains mobile hydrated cations, water as solvents, and fixed anions. When the IPMC is bent mechanically, the movement of inside hydrated cations toward the expanding region could produce output electrical signals between the two electrodes. The unique advantages of IPMC include self-powered and the identification of the bending direction by the direction of the generated electrical signals, which makes IPMC an ideal wearable sensor candidate. However, compared with a large amount of work conducted on the actuator field by many researchers, research of the IPMC as the sensor is relatively limited, and development of the stable IPMC structure as wearable sensor for the real-time monitoring of human-related activities has not been carried out so far. One of the possible reasons may be the easy evaporation of the water in the IPMC sensors, which could intensively affect the sensors stability and subsequently their further application development.[37]

Here we develop the piezoionic wearable sensors and realize the real-time detection of human activities ranging from large scale motions to subtle

physiological signals. First of all, we fabricate IPMC strain sensor by using ionic liquid (IL) as electrolyte instead of water. This sensor generates stable electrical voltage under the externally applied bending without the requirement of power supply, and the direction of the electrical signals can be changed with the variation of the bending direction. Under a bending-induced strain of 1.8%, an output voltage of 1.3 mV can be generated. Second, the long-time stability of the sensors in air is further realized by the parylene coating technique. On the basis of the IPMC structure, we further construct new piezoionic sensor by using graphene composite as the electrode to replace Au and realize greatly improvement of the voltage output. Finally, through simple encapsulation, the piezoionic sensor can be directly attached on human's skin or cloth for the real-time measurement of diverse human activities. The large scale wrist flex upward or downward, good or bad sitting posture, subtle pulse wave before and after strenuous exercise, and repeated finger touch can all be well monitored and distinguished, indicating the great potential of this wearable piezoionic sensor in the sensing applications from real time monitoring to portable friendly human-machine interaction.

2. Results and Discussion

The IPMC-structure piezoionic sensor studied here is fabricated by using an impregnation/reduction method that is originally proposed by Fujiwara et al. and subsequent thermal swelling of ionic liquid.[37,38] Here, ionic liquid is used as new electrolyte to replace water-solvent due to their high ion conductivity, high voltages stability, and nonvolatility. **Figure 1**a schematically describes the fabrication process. In brief, an ionic polymer membrane (Nafion) is placed into a solution of $[Au(Phen)Cl_2]Cl$ to allow the protons in the membrane to be exchanged with $[Au(Phen)Cl_2]^+$ ions. After that, these ions are reduced to Au on the surface of the membrane. Finally, ionic liquid is imbibed into the sample through a thermal swelling process. The details can be found in the Experimental Section. Figure 1b depicts the self-powered sensing mechanism of the piezoionic sensor. When the piezoionic sensor is

deformed mechanically, one side of the sensor is tensile while the other side is compressed. This imposed stress gradient causes the movement of the inside mobile ions from compressed regions to the expanding regions.[21,23] Because of the size differences between cations and anions, the ions movement is inhomogeneous. The imbalance of the ions distribution generates electrical signals output across the membrane thickness. Figure 1c gives the cross-sectional scanning electron microscopy (SEM) images of the IPMC structure, clearly indicating the uniform Au layer coated on the surface of the ionic polymer membrane layer and the tight binding of the two layers. In order to verify the layer coated on the ionic polymer membrane is Au, the energy-dispersive X-ray spectroscopy (EDX) signal is recorded and given in Figure 1d, which is collected from the layer in the red box in the inset SEM image. Au element can be clearly identified. Moreover, typical X-ray diffraction (XRD) powder diffraction pattern of the resulting surface layer of the IPMC is also shown in Figure 1e. The appeared four diffraction peaks on the XRD pattern of IPMC surface can be indexed to the (111), (200), (220), and (311) planes of the face-centered cubic gold crystal structure (JCPDS, File No. 04-0784), further demonstrating the existence of Au layer.

The sensing performance of the IPMC structure sensor upon mechanical bending is investigated, as shown in **Figure 2**. To realize the bending sensing detection, the sensor is suspended between the movable stage with the two ends fixed, and a step motor is used to drive back-and-forth translation of the movable stage. As shown in Figure S1a in the Supporting Information, the forth movement of the movable stage leads to the upward bending of the sensor membrane, while the back movement makes the bent sensor return to the flat state. Here, the free length of the IPMC sensor is 8 mm, and the maximum moving displacement of the movable stage is 3 mm. Because the sensing performance of the IPMC is related to the bending deformation, the bending-induced tensile strain on the outer surface relative to neutral axis of the membrane is employed to reflect the bending extent of the IPMC.

This tensile bending strain under the different displacement of the movable stage is calculated by using the software matlab based on Euler–Bernoulli beam theory when hypothesizes the neural axis of the membrane keeps its length during the bending and shown in Figure S1b in the Supporting Information.[13,15] An electrochemical station is connected to the two sides of the IPMC sensor to pick up the open circuit voltage. For the measurement, no voltage is applied on the IPMC sensor.

The sensing performance of the IPMC in response to the cyclic upward bending/flat is presented in Figure 2a. Under the mechanical bending of the IPMC sensor, an output voltage (1.3 mV) is clearly observed. It proves that the IPMC sensor only need mechanical deformation to generated electrical signals. Figure 2b gives the bending-induced strain of the IPMC under different time in one cycle (blue curve). The corresponding generated voltage signal is also given for comparison (red curve). With the increase of the strain, the voltage is also increased. This is attributed to the enlarged bending extent of the IPMC sensor thus the much more ions movement. When the strain is unchanged, a quasi-equilibrium ion distribution is reached. During the process, the imbalanced cation and anion gradually recombine, causing the slight decrease of the voltage. Moreover, the generated voltage of the IPMC as a function of the strain is also given (Figure 2c). An approximately linear relationship can be observed, which facilitates the sensing applications. Besides the open circuit voltage, short circuit current of the IPMC in response to the cyclic bending is also tested, as shown in Figure S2 in the Supporting Information. An output current of about 0.9 μA is generated under the same bending deformation. From the integration of each current peak, we could obtain that the charge transfer during operation is about 1 μC.

As the piezoresistive effect and triboelectric effect can also lead to the strain sensing, their possible influence on the sensing performance of the IPMC is investigated. Because both the piezoresistive effect and triboelectric effect are

irrelevant to the ions, the IPMC sensor without the inside ionic liquid is adopted for the test. For the piezoresistive sensing measurement, a 1 V external voltage is applied on the IPMC sensor, and the resistance variation under the cyclic bending deformation is simultaneously recorded (Figure S3, Supporting Information). The resistance change of the IPMC upon bending is nearly negligible ($<0.7\%$), revealing the piezoresistive effect has no obvious effect on the IPMC sensing. Moreover, the output electrical signals of the IPMC in response to the bending without ionic liquid is also measured. No voltage or current is generated under the bending, indicating that the IPMC response is indeed related to the ions, not resulted from the triboelectric effect.

To determine the response time, the IPMC sensor was applied with transient bending and the sensing response is simultaneously detected. Through the real-time record of the voltage–time curve (Figure S4, Supporting Information), the response time is determined to be around 50 ms. The fast response undoubtedly facilitates the real-time monitoring of fast and intricate human motions. Repeatability and stability of the sensors are extremely critical for practical application. For the purpose of testing the stability, repeatedly bending/ flat cycles are applied on the IPMC sensor by the stepper motor (displacement of 3 mm, 6 s for each cycle) and the generated voltage is simultaneously measured. As shown in Figure S5 in the Supporting Information, the response signal remained nearly unchanged after 400 cycles, revealing the high repeatability and stability.

Moreover, although ionic liquid used as the electrolyte in the sensors is nonvolatile compared to the water, there may be a little slow leakage of the ionic liquid after long time operation in air, which may have a certain impact on the sensor performance. Therefore, capsulation is still necessary for maintaining the device performance. Parylene is considered as the one of the most effective coating layer for the device capsulation.[39] Here, a commercial parylene coating machine is employed to deposit parylene on the IPMC sensors. Figure S6 (Supporting Information) shows the SEM image of the IPMC sensor deposited by the parylene with thickness of 1 μm. It can be seen that parylene is densely coated on the surface

of the IPMC sensor to form a smooth capsulation layer for the suppression of the ionic liquid loss. The lifetime of the sensor is largely increased after parylene coating. Placing in air for several months, the parylene coated sensors exhibit almost no degradation of the bending-generated sensing signals, which further provides the basis for the practical applications.

As we know, the generated electrical signals are intensively dependent on the contact areas between electrode layers and ionic polymer interlayer. [23,40,41] Therefore, the electrode design is crucial to the performance of the piezoionic sensor. In our previous work, various nanomaterials including graphene and carbon nanotube (CNT) are employed as the electrode materials for the construction of ionic actuators which exhibit attractive high-performance actuation responses.[42–44] Inspired by previous studies, graphene and CNT, which have large specific surface area and excellent properties, are also used to form the piezoionic sensors. **Figure 3**a gives the SEM image of the graphene/CNT electrode, which shows the porous structure. Under cyclic bending of the graphene-based piezoionic sensor, a voltage of about 4.5 mV is generated (Figure 3b), which is larger than the voltage generated by the IPMC sensor with Au electrode. For a better comparison, the curves of the generated voltage versus the applied bending strain for both the piezoionic sensors with graphene based electrode and Au electrode are also shown in Figure 3c. Under the same bending strain, the voltage generated by sample with graphene based electrode is largely increased. This may be attributed to the large specific surface area of the graphene based electrode which is beneficial for the generation of larger mechanical-to-electrical signals.[40,41] For this ionic type sensor, the electrical signals are related to the number of mobile ions at the electrodes. A higher population of charged ions at the electrodes is preferred for sensing performance. The graphene based electrodes with large specific surface area provide large contact areas with ionic polymer interlayer, which is capable of reserving more ions. When a bending deformation is applied, a larger number of ions can be accumulated at the electrode, resulting in the generation of larger electrical signals. Furthermore, the output voltage of the graphene based

sensor with different specific surface area is also given (Figure S7, Supporting Information). Larger specific surface area leads to higher voltage, which further confirms the great influence of the specific surface area from the graphene based electrode.

The great potential of the IPMC structure piezoionic sensor as wearable sensor toward monitoring of diverse human activities is also investigated. To construct a wearable sensor, the IPMC sensor with the two sides connected to the electrical wires respectively by the conductive silver adhesives is covered with two layers of the acrylic elastomer (VHB, 3M). Very high bond (VHB) is marketed as a double-sided adhesive tape. Because of the pronounced viscoelastic behavior VHB has, this simple encapsulation is beneficial for the protection of the sensor as well as integration with human's skin and clothing. Figure 4 shows the wearable sensor for the monitoring of large scale human motions. As shown in Figure 4 a, the wearable sensor is directly attached to the back of a person's wrist joint. The wrist joint bending trail (marked from (1) to (5) in Figure 4 a), including the bending direction and amplitude, can be detected and distinguished through the electrical signals generated by the sensor. Another important usage for this wearable sensor is the sitting posture monitoring. As we know, spine is a very important part of the human body. For the person who works at desk for long time, a good sitting posture is crucial to protecting the health of the spine. Figure 4 b shows that the wearable sensor attached on the person's back succeeds in detecting the sitting posture change from good to bad (marked (1) and (2) in Figure 4 b).

Besides the large scale motion monitoring, this wearable sensor can be used for detecting the subtle physiological signals. A typical example is the pulse wave monitoring. Pulse wave is an important physiological signal for the arterial

blood pressure and heart rate. After adhere to the wrist (**Figure 5**a), the voltage signal of the wearable sensor before and after exercise is recorded (Figure 5b). The amplitude and frequency of pulse wave can be read out readily in real time. It shows clearly that the normal pulse frequency of the person is 83 beats per min with regular and repeatable pulse shape, and this pulse frequency after strenuous exercise increases to 107 beats per min with a little enhancement of the intensity. In addition to wearable sensing for humans, the tactile sensing is also realized by this sensor. As shown in Figure 5c, the flexible sensor is adhered to the back of the hand. When using finger to lightly touch the sensor, voltage (Figure 5d) is generated. The touch times can be clearly observed from the generated electrical signals. Particularly, the electrical voltage is produced only by the mechanical touch. The well tactile sensing performance with self-powered property reveals the great prospect of the piezoionic sensor for the friendly human-machine interactive applications.

3. Conclusion

Piezoionic sensors based on Au electrode as well as graphene composite electrode are both fabricated. These sensors could generate electrical signals in response to the mechanical bending without the electric power supply, and the bending direction and amplitude can be clearly discriminated. The Au electrode piezoionic sensor can generate an output voltage of 1.3 mV under a bending-induced strain of 1.8%. When the graphene composite is employed as the electrode to replace Au electrode, the generated voltage of the piezoionic sensor is largely improved, which may be due to the large specific surface area and contact area with ionic liquid brought by the graphene electrode. This piezoionic sensor is assembled into wearable senor and succeeds in the real-time monitoring of human activities from large scale motions to subtle physiological signals, including wrist bending with different directions, sitting posture variation from good to bad, pulse wave before and after strenuous exercise, and the tactile sensing by the finger touch. These remarkable performances reveal the great prospective of the wearable piezoionic sensor for widely applications from the real time monitoring of human motion to further

portable human-machine interaction systems.

4. Experimental Section

Materials: Natural graphite flake (325 meshes, 99.8%, ABCR GmbH & Co. KG) was obtained from Sigma–Aldrich. Hydrogen peroxide, sulfuric acid, $HAuCl_4$, 1,10-Phenanthroline monohydrate (Phen), N-methyl-2-pyrrolidone (NMP), thermoplastic polyurethanes (TPU), and dimethylacetamide (DMAC) were purchased from Sinopharm Chemical Regent Co. Ltd. Single-walled carbon nanotubes were purchased from NJXF TECH Co. Ltd. Nafion 117 membrane was purchased from the Dupont. The used ionic liquid was 1-ethyl-3-methylimidazolium *bis*(trifluoromethylsulfonyl) imide (EMITFSI) which was purchased from SCJC Co. Ltd.

Preparation of the IPMC Sensor: Metal Au was deposited on the Nafion membrane by an impregnation/reduction method.[45,46] First, hydrogen peroxide (5% mass fraction) and diluted sulfuric acid (1 mol L^{-1}) were used to make the Nafion membrane clean. Then, the membrane was placed into a solution of $[Au(Phen)Cl_2]Cl$ which is precast by chemical synthesis[47] for 24 h to allow the sufficient impregnation of cations. After that, the Nafion membrane was immersed into deionized water in water-bath heating. A Na_2SO_3 solution of 5 mmol L^{-1} was slowly dropped into the water till the Au cation at the membrane's surface was reduced to metallic Au totally. This impregnation/reduction step was repeated to get a better surface conductivity of the Au electrode.[40] After that, the IPMC membrane was placed into the ionic liquid (EMITFSI) solution at 120 °C for 2 h to let the sample impregnated with ionic liquid, obtaining the IPMC sensor. The residual ionic liquid on the surface was removed with a clean filter. The IPMC sensor is cut into a size of 8 mm × 4 mm for the experimental test.

Fabrication of the Graphene Based Piezoionic Sensor: The graphene based piezoionic sensors were fabricated by layer-by-layer casting and hot-pressing method. Graphene oxide (GO) was prepared following the typical chemical method and has been described in our recent work.[48,49] The hybrid GO/CNT with the weight ratio of 3:1 was obtained by

dispersing CNT in GO solution for 200 W 20 kHz horn sonication treatment in a program of 2 s on and 5 s off for 30 min under ice water bath. The GO/CNT dispersion was then reduced to RGO (reduced graphene oxide)/CNT with N_2H_4 in a 90 °C oil bath.[48] After centrifugation, filtration, and washing with deionized water, the RGO/CNT were redispersed using the same sonication program in NMP, forming gel-like suspension of 1 mg mL^{-1} RGO/CNT. Mixture of TPU and IL was obtained by dispersing TPU and IL in DMAC solution with sonication. The as-prepared 2 mL RGO/CNT suspension was casted on glass slide substrate (7.5 cm × 2.5 cm) and gradually heated at 40 °C to prepare the RGO/CNT hybrid membrane electrode. Before the RGO/CNT membrane was completely dry, the IL/TPU mixture was casted on the electrode membrane to form the bilayer membrane, which was then dried at 60 °C. Two pieces of the bilayer membrane were hot-pressed at 170 °C for 4 h to obtain the graphene electrode based piezoionic sensor. The change of the specific surface area of the RGO/CNT membrane electrode is realized through changing the weight ratio of RGO and CNT.

Sensing Measurement: The piezoionic membrane sensor was placed between the motorized translation stages (Beijing Optical Century Instrument Co.,LTD. MTS121) with the two ends fixed. The free length of the membrane was 8 mm. Computer-controlled step motor was used to control the displacement and the deformation times of the membrane. The displacement of the movable stage under the different time was recorded by the laser displacement sensor (Keyence, LK-G80). The sensor was connected to an electrochemical workstation (CHI900D) with the two sides. The output electrical signals from the sensors were directly collected by the CHI 900D electrochemical workstation and agilent B1500A semi-conductor device analyzer.

Characterization: SEM images were performed with Hitach S-4800 filed emission scanning electron microscope. EDX was taken on Quanta 400FEG (FEI). XRD patterns were obtained on X'Pert-Pro MPD (Cu-Ka). Parylene coating was performed by the parylene vacuum gas phase film coating machine (PTP-3V, Penta Technology (Suzhou) Co., Ltd).

Supporting Information

Supporting Information is available from the Wiley Online Library or from the author.

Acknowledgements

Y.L. and Y.H. contributed equally to this work. The authors acknowledge the Hong Kong, Macao, and Taiwan Science & Technology Cooperation Program of China (Grant No. 2012DFH50120), the National Natural Science Foundation of China (Grant Nos. 11204350 and 21373263), the Natural Science Foundation of Jiangsu Province (Grant No. BK20131173), the External Cooperation Program of BIC, the Chinese Academy of Science (Grant No. 121E32KYSB20130009), and the Special Project of Nanometer Technology in Suzhou (ZXG201423).

Reference

[1] W. Zeng , L. Shu , Q. Li , S. Chen , F. Wang , X. M. Tao , Adv. Mater. 2014, 26 , 5310 .

[2] D. J. Lipomi , M. Vosgueritchian , B. C. K. Tee , S. L. Hellstrom , J. A. Lee , C. H. Fox , Z. Bao , Nat. Nanotechnol. 2011 , 6 , 788 .

[3] T. Yamada , Y. Hayamizu , Y. Yamamoto , Y. Yomogida , A. I. Najafabadi , D. N. Futaba , K. Hata , Nat. Nanotechnol. 2011 , 6 , 296 .

[4] C. Pang , G. Y. Lee , T. I. Kim , S. M. Kim , H. N. Kim , S. H. Ahn , K. Y. Suh , Nat. Mater. 2012 , 11 , 795 .

[5] A. Keshavarzi , M. Shahinpoor , K. J. Kim , J. Lantz , Part of the SPIE Conference on Electroactive Polymer Actuators and Devices , Newport Beach , California , March 1999 .

[6] S. Jung , J. Lee , T. Hyeon , M. Lee , D. H. Kim , Adv. Mater. 2014 , 26 , 6329 .

[7] S. Gong , W. Schwalb , Y. Wang , Y. Chen , Y. Tang , J. Si , B. Shirinzadeh , W. Cheng , Nat. Commun. 2014 , 5 , 3132 .

[8] C. M. Boutry , A. Nguyen , Q. O. Lawal , A. Chortos , S. RondeauGagné , Z. Bao , Adv. Mater. 2015 , 27 , 6954 .

[9] C. S. Boland , U. Khan , C. Backes , A. O'Neill , J. McCauley , S. Duane , R.

Shanker , Y. Liu , I. Jurewicz , A. B. Dalton , J. N. Coleman , ACS Nano 2014 , 8 , 8819 .
[10] X. Wang , Y. Gu , Z. Xiong , Z. Cui , T. Zhang , Adv. Mater. 2014 , 26 , 1336 .
[11] S. Y. Kim , S. Park , H. W. Park , D. H. Park , Y. Jeong , D. H. Kim , Adv. Mater. 2015 , 27 , 4178 .
[12] J. J. Park , W. J. Hyun , S. C. Mun , Y. T. Park , O. O. Park , ACS Appl. Mater. Interfaces 2015 , 7 , 6317 .
[13] Y. Cheng , R. Wang , J. Sun , L. Gao , Adv. Mater. 2015 , 27 , 7365 .
[14] B. Hwang , J. Lee , T. Q. Trung , E. Roh , D. Kim , S. Kim , N. Lee ACS Nano 2015 , 9 , 8801 .
[15] X. Liao , Q. Liao , X. Yan , Q. Liang , H. Si , M. Li , H. Wu , S. Cao , Y. Zhang , Adv. Funct. Mater. 2015 , 25 , 2395 .
[16] M. S. U. Sarwar , Y. Dobashi , E. F. S. Glitz , M. Farajollahi , S. Mirabbasi , S. Nafi ci , G. M. Spinks , J. D. W. Madden , Proc. SPIE 2015 , 9430 , 943026 .
[17] W. Takashima , T. Uesugi , M. Fukui , M. Kaneko , K. Kaneto , Synth. Met. 1997 , 85 , 1395 .
[18] T. Shoa , J. D. W. Madden , T. Mirfakhrai , G. Alici , G. M. Spinks , G. G. Wallace , Sens. Actuators A 2010 , 161 , 127 .
[19] Y. Wu , G. Alici , J. D. W. Madden , G. M. Spinks , G. G. Wallace , Adv. Funct. Mater. 2007 , 17 , 3216 .
[20] G. Alici , G. M. Spinks , J. D. Madden , Y. Wu , G. G. Wallace , IEEE/ASME Trans. Mechatronics 2008 , 13 , 187 .
[21] M. Shahinpoor , Proc. SPIE 1995 , 2441 , 42 .
[22] B. Bhandari , G.-Y. Lee , S.-H. Ahn , Int. J. Precis. Eng. Man. 2012 , 13 , 141 .
[23] M. Shahinpoor , Y. Bar-Cohen , J. O. Simpson , J. Smith , Smart Mater. Struct. 1998 , 7 , 15 .
[24] Z. L. Wang , J. Song , Science 2006 , 312 , 242 .
[25] F. Fan , Z. Tian , Z. L. Wang , Nano Energy 2012 , 1 , 328 .
[26] K. C. Pradel , W. Wu , Y. Ding , Z. L. Wang , Nano Lett. 2014 , 14 , 6897 .
[27] J. Zhong , Y. Zhang , Q. Zhong , Q. Hu , B. Hu , Z. L. Wang , J. Zhou , ACS Nano 2014 , 8 , 6273 .
[28] W. Seung , M. K. Gupta , K. Y. Lee , K. Shin , J. Lee , T. Kim , S. Kim , J. Lin , J.

H. Kim , S. Kim , ACS Nano 2015 , 9 , 3501 .
[29] M. Shahinpoor , K. J. Kim , Smart Mater. Struct. 2000 , 9 , 543 .
[30] M. Shahinpoor , K. Kim , Smart Mater. Struct. 2001 , 10 , 819 .
[31] K. J. Kim , M. Shahinpoor , Smart Mater. Struct. 2003 , 12 , 65 .
[32] M. Shahinpoor , Electrochim. Acta 2003 , 48 , 2343 .
[33] M. Shahinpoor , K. J. Kim , Smart Mater. Struct. 2004 , 13 , 1362 .
[34] M. D. Bennett , D. J. Leo , G. L. Wilkes , F. L. Beyer , T. W. Pechar , Polymer 2006 , 47 , 6782 .
[35] K. Park , H. Lee , J. Korean Phys. Soc. 2012 , 60 , 821 .
[36] D. Pugal , K. Jung , A. Aabloo , K. J. Kim , Polym. Int. 2010 , 59 , 279 .
[37] M. D. Bennett , D. J. Leo , Sens. Actuators A 2004 , 115 , 79 .
[38] N. Fujiwara , K. Asaka , Y. Nishimura , K. Oguro , E. Torikai , Chem. Mater. 2000 , 12 , 1750 .
[39] S. J. Kim , I. T. Lee , H. Lee , Y. H. Kim , Smart Mater. Struct. 2006 , 15 , 1540 .
[40] K. Onishi , S. Sewa , K. Asaka , N. Fujiwara , K. Oguro , Electrochim. Acta 2001 , 46 , 737 .
[41] B. J. Akle , D. J. Leo , M. A. Hickner , J. E. McGrath , J. Mater. Sci. 2005 , 40 , 3715 .
[42] L. Lu , J. Liu , Y. Hu , Y. Zhang , H. Randriamahazaka , W. Chen ,Adv. Mater. 2012 , 24 , 4317 .
[43] G. Wu , G. Li , T. Lan , Y. Hu , Q. Li , T. Zhang , W. Chen , J. Mater. Chem. A 2014 , 2 , 16836 .
[44] G. Wu , Y. Hu , Y. Liu , J. Zhao , X. Chen , V. Whoehling , C. Plesse , G. T. M. Nguyen , F. Vidal , W. Chen , Nat. Commun. 2015 , 6 , 7528 .
[45] N. Fujiwara , K. Asaka , Y. Nishimura , K. Oguro , E. Torikai , Chem. Mater. 2000 , 12 , 1750 .
[46] K. J. Kim , M. Shahinpoor , Smart Mater. Struct. 2003 , 12 , 65 .
[47] C. M. Harris , J. Chem. Soc. 1959 , 682 .
[48] D. Li , M. B. Muller , S. Gilje , R. B. Kaner , G. G. Wallace , Nat. Nano-technol. 2008 , 3 , 101 .
[49] J. Liu , Z. Wang , L. Liu , W. Chen , Phys. Chem. Chem. Phys. 2011 , 7 , 13216 .

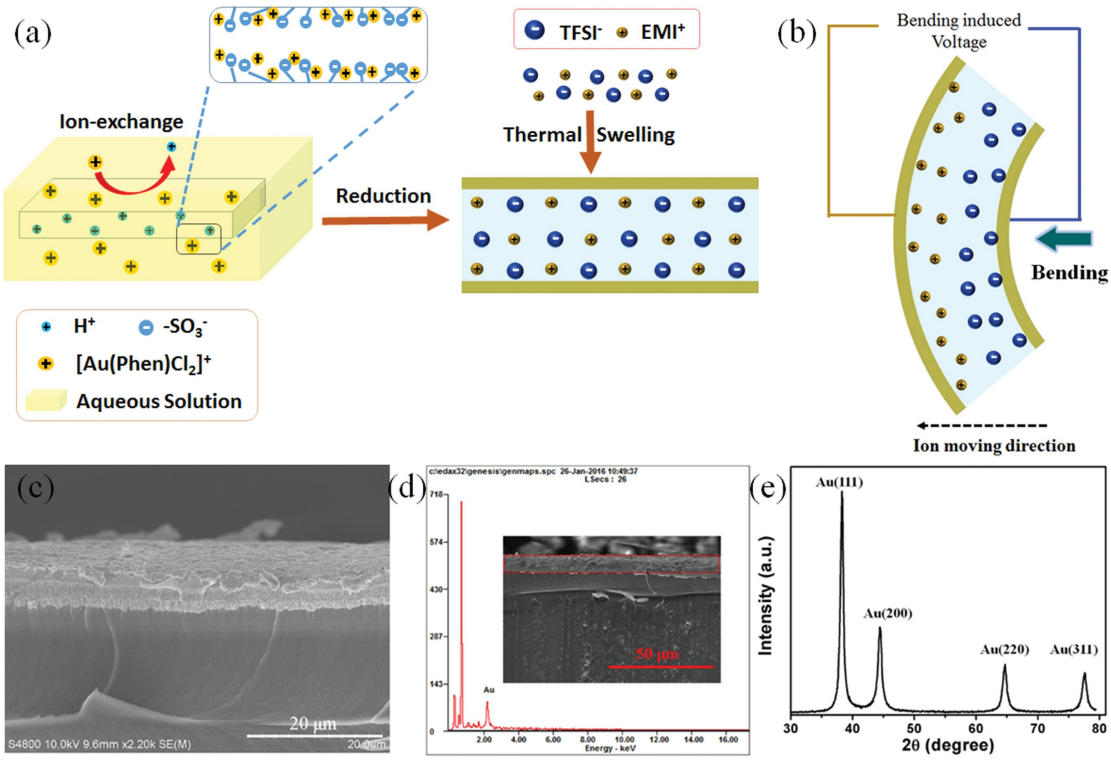

Figure 1. a) Schematic diagram of the fabrication process of the IPMC piezoionic sensor. b) Schematic diagram for the mechanism of the self-powered sensing in piezoionic strain sensor due to redistribution of the ions. c) Cross-sectional SEM image of the IPMC showing the electrode-polymer interface. d) EDX (energy dispersive X-ray) analysis of the IPMC. The inset shows the corresponding SEM image. e) XRD patterns of the IPMC. The peaks at 38°, 44°, 64°, and 77° correspond to the (111), (200), (220), and (311) crystalline planes of Au, respectively.

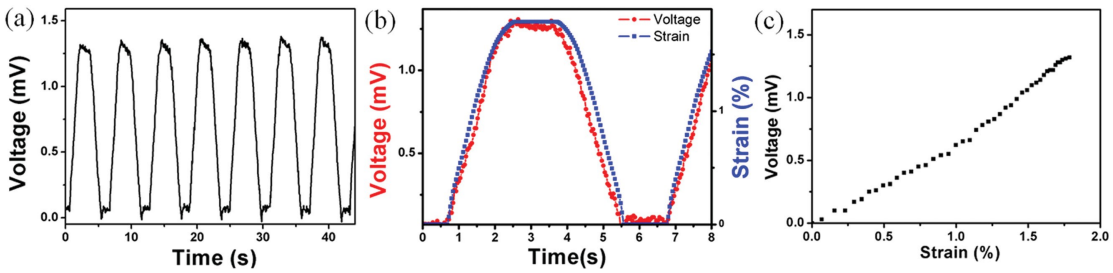

Figure 2. a) Electrical response of the IPMC strain sensor under the cyclic uniaxial movement induced bending. b) Strain change of the IPMC sensor (blue curve) and the simultaneously generated voltage variation (red curve). c) Voltage variation of the IPMC sensor with the different bending strain.

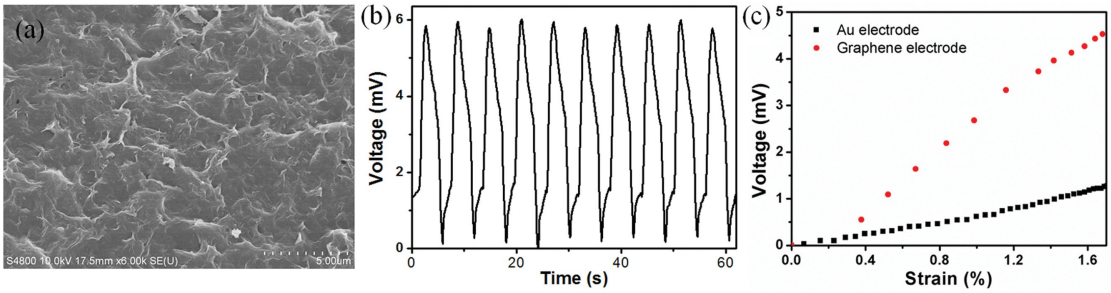

Figure 3. Response of the graphene-based piezoionic sensor. a) SEM image of the graphene composite electrode. b) Generated voltage of the graphene-based piezoionic sensor in response to the cyclic bending. c) Voltage as a function of the bending induced strain for the IPMC piezoionic sensors with different electrode (red curve refers to graphene based electrode, while black curve is Au electrode).

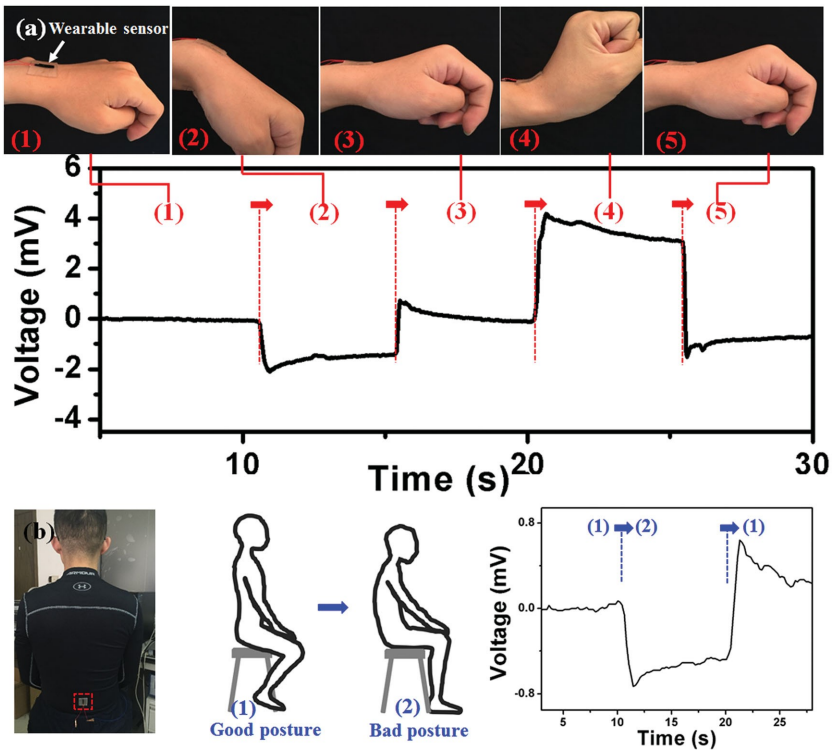

Figure 4. Applications of the piezoionic sensor as wearable sensor for the monitoring of large scale human motions. a) Response signals of the wearable sensor for monitoring of the wrist bending with different directions. The photographs show that wearable sensor is attached on

the wrist joint and the wrist joint moving process started from the flat state (1) to the finally flat state (5). The generated voltage indicates that the direction as well as the amplitude ofthe wrist bending can be clearly detected and distinguished. b) Monitoring of the person's sitting posture by this wearable sensor. The wearable sensor is attached to the person's back,marked in the red box in the photograph. When the person's sitting posture is from good(marked as (1)) to bad (marked as (2)), the sensor could generate clear electrical signal in response to the change

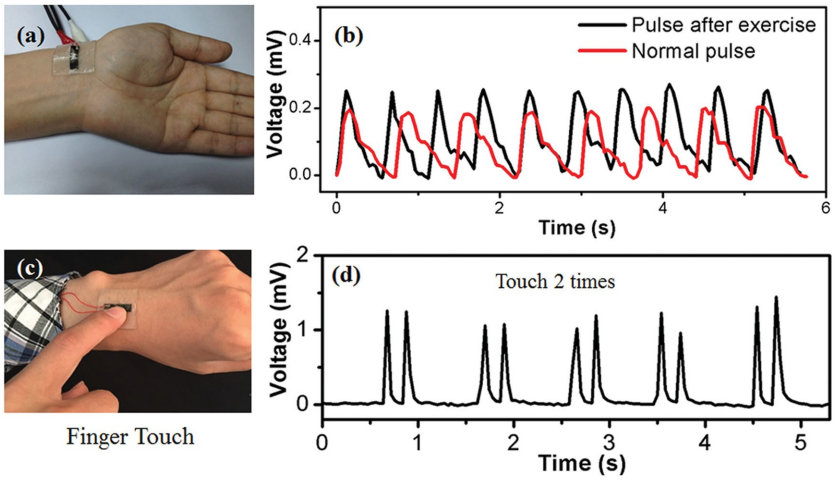

Figure 5. a) Photograph of wearable sensor directly attached to the wrist. b) Voltage response of the wearable sensor on the wrist before and after exercise. c) Photograph of wearable sensor attached to the back of the hand for the finger touch sensing. d) Generated voltage of the wearable sensor in response to the cyclic 2 times finger touch.